Fragmentation path for hydrogen atom dissociation from methoxy radical

Nicholas D. K. Petraco, Wesley D. Allen, and Henry F. Schaefer III
Center for Computational Quantum Chemistry, University of Georgia, Athens, Georgia 30602-2525

(Received 2 January 2002; accepted 19 March 2002)

Salient features of the potential surface for hydrogen atom dissociation from the methoxy radical (CH_3O) have been investigated via high-level coupled-cluster methods using a TZ2P(f,d) basis set for geometry optimization and harmonic vibrational analyses and the correlation-consistent cc-pVXZ ($X=2-6$) series for final energetic determinations and extrapolations. Of central concern for continuing photofragmentation dynamics experiments is the C_s-symmetry $^2A'$ transition state for dissociation, which TZ2P(f,d) RCCSD(T) theory locates at a critical C–H distance of 1.79 Å with a barrier frequency of $947i$ cm^{-1}. Our zero-point-corrected focal-point extrapolations place this transition state 4.7 kcal mol^{-1} above the CH_2O+H products and yield a dissociation energy of 20.1 kcal mol^{-1}; the latter differs from the most reliable experimental values by only 0.2–0.3 kcal mol^{-1}. A revised enthalpy of formation, $\Delta H^{\circ}_{f,0}(CH_3O)=6.5$ kcal mol^{-1}, is proposed. Disappointingly, TZ2P(f,d) UB3LYP theory underestimates the CH_2O+H association barrier by 2.3 kcal mol^{-1}, missing about half the barrier height. The complete set of TZ2P(f,d) RCCSD(T) data for structures and frequencies coupled with final focal-point energetics provides definitive values for parameters essential to the analysis of experimental photofragmentation rate profiles. © *2002 American Institute of Physics.* [DOI: 10.1063/1.1477180]

I. INTRODUCTION

Since its discovery in 1953, the methoxy radical has become one of the most widely studied organic radicals.[1,2] This species, which turns up in many fields of chemistry, is preeminent in atmospheric and combustion chemistry, being an intermediate in methane and other flames as well as an important component of smog.[3–7] Methoxy generally appears in the photochemical oxidation of hydrocarbons and contributes to the presence of HO_2 radicals in the atmosphere.[8,9] The CH_3O radical is also believed to aid in the conversion of NO to NO_2 in polluted atmospheres.[10]

Recent experimental work has made the methoxy radical a fertile testing ground for unimolecular chemical dynamics, including intramolecular vibrational energy redistribution (IVR) and related, fundamental theories of reaction rates such as Rice-Ramsperger-Kassel-Marcus (RRKM) theory.[11–16] Osborn *et al.*[17,18] recently studied the photofragmentation dynamics of methoxy at wavelengths in the 250–285 nm range. After excitation to the $\tilde{A}^2A_1$ state, they observed that the major fragmentation product channel was CH_3+O; however, at these high excitation energies, the thermodynamically preferred hydrogen-atom dissociation, ensuing on the ground-state surface, occurred 2%–10% of the time.[18] Particularly intriguing is the accessibility of the threshold for $CH_3O\rightarrow CH_2O+H$ bond dissociation within 25 kcal mol^{-1} of the ground vibrational state of methoxy, facilitating detailed experimental probes of the interplay between statistical behavior and state-specific quantum dynamics over a fragmentation barrier of unusually low energy.[19] Controlled methoxy fragmentation at relatively low energies can be achieved using lasers in a stimulated emission pumping scheme, whereby the molecule is first pumped to the higher $\tilde{A}^2A_1$ electronic state and then dumped to selected excited vibrational levels on the ground surface in the vicinity of the hydrogen dissociation barrier.[19,20] As demonstrated in other systems such as ketene[21–25] and acetaldehyde,[26,27] tuning the imparted vibrational excitation energy through the threshold region and upward reveals a spectroscopic signature with a wealth of dynamical information. The interpretation of these signatures can be difficult and controversial,[21–27] but in their elucidation groundbreaking insights may be revealed for the attendant reaction dynamics. In such cases it is imperative that the system be rigorously analyzed by electronic structure theory and that the necessary features of the potential surface be definitively established by *ab initio* investigations.

In C_{3v} symmetry, the methoxy radical has a ^2E electronic ground state, which is subject to Jahn–Teller (JT) distortions along the e vibrational modes, splitting the degeneracy into a ($^2A'$,$^2A''$) pair of states differing in orbital occupancy by a $(2a'')^2(7a')\rightarrow(2a'')(7a')^2$ excitation. In this classic Jahn–Teller system,[28,29] the $^2A'$ state is known to be the lowest state in C_s symmetry, while its $^2A''$ companion comprises the saddle points for interconversions of equivalent $^2A'$ minima in the threefold pseudorotation well. Previous computations indicate that the ($^2A'$,$^2A''$) energy splitting is only about 0.11 kcal mol^{-1} and the JT stabilization energy from the ^2E state is merely 0.60 kcal mol^{-1}.[30] However, despite much theoretical work,[30–41] questions have persisted regarding the intricate JT pseudorotation surface and its extension into the dissociation channels, including some disagreement in the experimental literature[19,20,42–50] as to the structure and spectroscopy of the ^2E surface. In the region near the CH_3O equilibrium, notable aid has come from a very recent MRCI study[30] which computed both sheets of the $\tilde{X}^2E$ electronic state and performed dynamical calculations for the vibronic structure. Nonetheless, experimental efforts

to observe state-specific reaction dynamics in the dissociation channels continue to be hindered by complexities resulting from the Jahn–Teller characteristics of the methoxy radical. In support of ongoing photofragmentation studies of the methoxy radical, we present here high-level coupled-cluster structural, energetic, and vibrational frequency predictions for the hydrogen atom dissociation path, with emphasis on the C_s-symmetry $^2A'$ transition state.

II. COMPUTATIONAL METHODS

Electronic energies were obtained using both spin-restricted and spin-unrestricted Hartree-Fock (ROHF, UHF) reference wave functions.[51–54] Post Hartree-Fock correlation methods included second-order Møller-Plesset perturbation theory (MP2),[51,52,55,56] the coupled-cluster singles and doubles method (CCSD),[57–60] and CCSD method augmented either by full[61–63] or perturbative[64,65] inclusion of connected triple excitations [CCSDT or CCSD(T)]. The lowest two occupied and highest two unoccupied orbitals were frozen in all dynamical correlation procedures. All coupled-cluster results were obtained with the ACESII program package.[66] For comparison purposes, density functional theory was also employed using the three-parameter HF/DFT hybrid Becke exchange functional with the correlation functional of Lee, Yang, and Parr (B3LYP).[67,68] Spin restriction was not imposed on the DFT calculations. All Hartree-Fock and DFT results were obtained with the GAUSSIAN program suite.[69]

Two basis sets were employed in geometry optimizations for this study. For exploratory computations, a DZP basis was constructed from a standard Huzinaga-Dunning *sp* set[70–72] of contracted Gaussian functions (CGFs) augmented with correlation-optimized polarization functions taken from the cc-pVDZ basis sets.[73] The contraction scheme for the DZP set was H($4s1p/2s1p$) and C,O($9s5p1d/4s2p1d$), with 45 total CGFs. For final structures, a TZ2P(f,d) basis was formed from larger Huzinaga-Dunning *sp* sets[70,74] augmented with ($2d1f,2p1d$) correlation-optimized polarization manifolds from the cc-pVTZ sets.[73,75] The contraction scheme for the TZ2P(f,d) basis was H($5s2p1d/3s2p1d$) and C,O($10s5p2d1f/4s3p2d1f$), with 104 CGFs. All polarization manifolds used in this study were comprised only of pure spherical harmonics. Stationary points were optimized within C_s (reactant, transition state) or C_{2v} (product) symmetry using analytic gradient techniques,[76–78] until all residual Cartesian gradients were less than 10^{-6} a.u. Quadratic force constants for Hartree-Fock (HF) and density functional theory (DFT) were determined via analytic second derivatives. The coupled-cluster force constants were determined using analytic gradients by means of careful finite difference techniques.

Focal-point energetic analyses[79–83] and extrapolations were performed using UHF-based correlation energies at the TZ2P(f,d) UCCSD(T) optimized geometries, all computations again utilizing the ACESII program package. Complete basis set (CBS) limits for the focal-point scheme were surmised from sequences of cc-pVXZ computations[73,84–86] through $X=6$, involving as many as 553 functions. The analytic forms adopted for the extrapolations were

$$E_{\mathrm{UHF}}(X)=E_{\mathrm{UHF}}^{\infty}+ae^{-bX} \tag{1}$$

and

$$E_{\mathrm{corr}}(X)=E_{\mathrm{UMP2,UCC}}(X)-E_{\mathrm{UHF}}(X)=E_{\mathrm{corr}}^{\infty}+bX^{-3}, \tag{2}$$

which are based on both theoretical considerations and extensive computational observations.[79,87–91]

III. FEATURES OF THE HYDROGEN DISSOCIATION PATH

A. Stationary structures

Figure 1 presents the geometric structures optimized in the current investigation for the ($^2A',^2A''$) ground-state manifold of CH_3O, the $^2A'$ transition state for H-atom extrusion, and the formaldehyde product. Table I compares these predictions with analogous structures determined in the best previous *ab initio* work.[30,33,34,36,41,92] The summary in Table I shows general consistency among theoretical data but an unsatisfactory lack of convergence in geometric parameters, due to limitations both in the basis sets and in the dynamical electron correlation treatments. The comparisons in the table will not be belabored here, except for discussing below the striking disparities in R(C–H) for the transition state; rather, focus will be given to our results obtained with the TZ2P(f,d) RCCSD(T) method, whose reliability is thoroughly established in the literature.[93–96]

In the ($^2A',^2A''$) ground-state manifold of methoxy, the C–O distances (1.3746 ± 0.0006 Å) are contracted about 0.05 Å compared to methanol, while the C–H distances, averaging 1.1053 Å, are roughly 0.01 Å longer than in CH_3OH.[97] At the TZ2P(f,d) RCCSD(T) level, Jahn–Teller distortions in the lower-energy $^2A'$ state of CH_3O yield a unique C–H distance 0.0060 Å longer and a pair of C–H distances 0.0027 Å shorter than the overall ($^2A',^2A''$) average. In contrast, the $^2A''$ component, lying 51 cm^{-1} higher (vide infra Table III), displays a pair of C–H distances 0.0018 Å longer and a unique C–H distance 0.0042 Å shorter than the same average. In the $^2A'$ state, the unique and symmetry-equivalent H–C–H angles deviate by $+3.2°$ and $-1.6°$, respectively, from the overall mean of 108.4°. By comparison, the companion $^2A''$ structure has corresponding unique and symmetry-equivalent H–C–H angle deviations of $-3.6°$ and $+1.8°$, respectively. Finally, in the ($^2A',^2A''$) structures, the C–O axis is tilted (toward, away from) the unique hydrogen atom. The shallowness of the pseudorotation potential well and concomitant zero-point vibrational averaging have precluded experimental determinations of Jahn–Teller distorted structures of CH_3O. For example, submillimeter wave spectroscopy has given an effective C_{3v} r_s structure, r(C–H) $=1.1176$ Å, r(C–O)$=1.39258$ Å, and $\angle$(H–C–O) $=113.9°$,[98] yet all of these values appear to be too large in relation to the average TZ2P(f,d) RCCSD(T) parameters in Fig. 1.

The optimum ($^2A',^2A''$) methoxy structures given for other levels of theory in Fig. 1 exhibit varying degrees of agreement with the TZ2P(f,d) RCCSD(T) standards. For both states, the UHF spin contamination is less than 0.01 a.u. and accordingly, all (U,R) pairs of coupled-cluster geometric parameters agree remarkably, to 0.0001 Å and 0.01°. For the

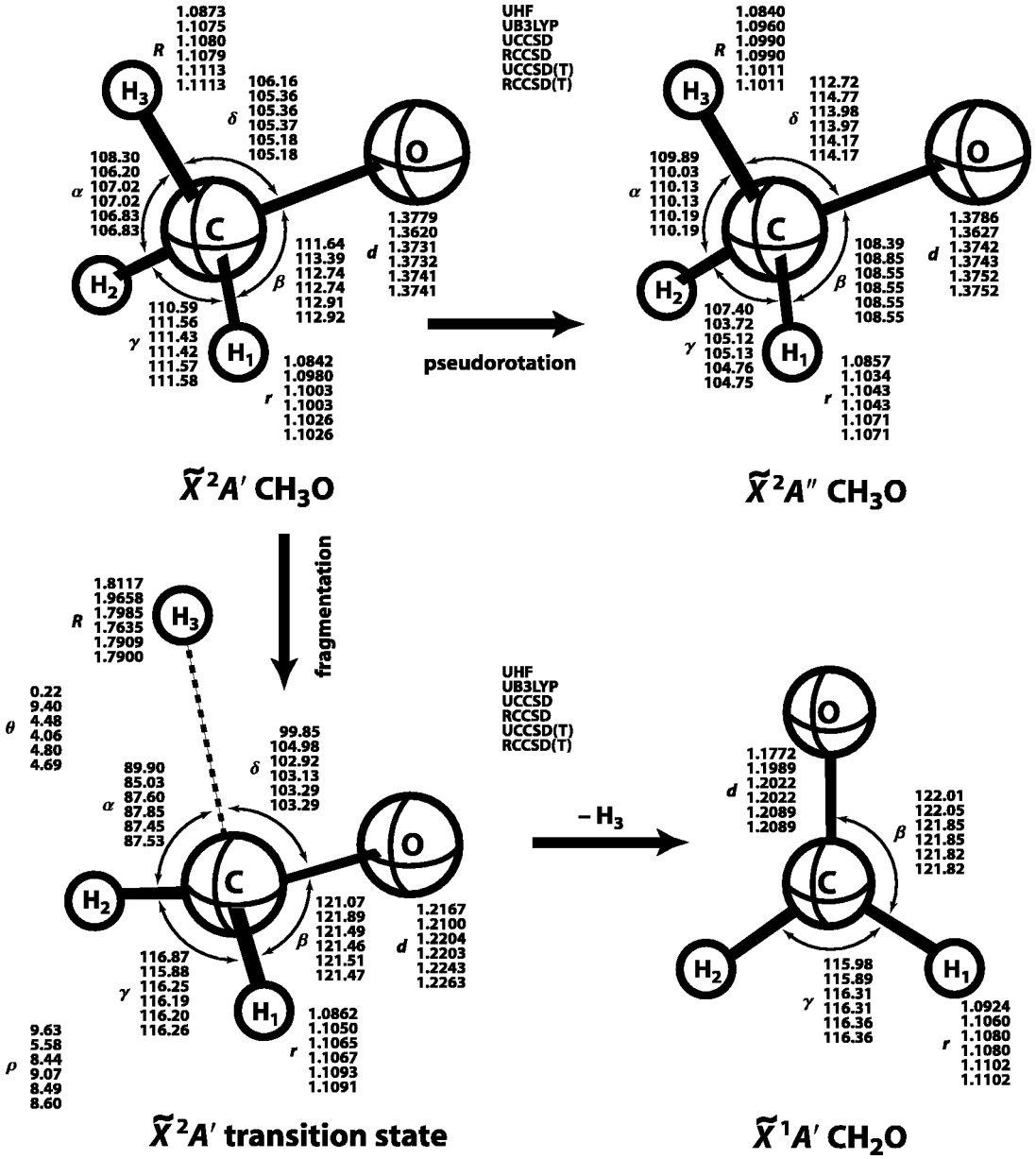

FIG. 1. TZ2P(f,d) stationary structures for the hydrogen-atom dissociation path of methoxy radical. Sets of optimized [UHF, UB3LYP, UCCSD, RCCSD, UCCSD(T), RCCSD(T)] bond distances (Å) and angles (deg) are shown for each coordinate. The fragmentation and pseudorotation processes maintain C_s symmetry with respect to the H_3–C–O reflection plane. For the transition state, the angle (ρ) of the C–O bond out of the H_1–C–H_2 plane is given by $\cos\rho = -\cos\beta\ \sec(\gamma/2)$, and the deflection angle (θ) of the C–H_3 vector from the normal to the same plane is defined as $\theta = \delta - \rho - 90°$.

C–H bond lengths, typical trends are seen within the UHF→CCSD→CCSD(T) series, viz., successive shifts of $+0.018\pm0.003$ Å and $+0.0027\pm0.0007$ Å, whereas the corresponding UB3LYP values lie below but within 0.003 Å of the CCSD predictions. For the C–O bond, it is unusual that the UHF r_e value is 0.003–0.005 Å larger than the CCSD and CCSD(T) bond lengths (which agree within 0.001 Å), while the UB3LYP method gives the poorest result, 0.012 Å shorter than CCSD. Among the bond angles shown in Fig. 1, the (average absolute, largest) changes for UHF→CCSD, UB3LYP→CCSD, and CCSD→CCSD(T) are (1.0°,−2.3°), (0.5°,+1.4°), and (0.2°,−0.4°), respectively, with $\gamma(^2A'')$ consistently being the angle of greatest sensitivity. With regard to the magnitude of the aforementioned Jahn–Teller distortions from overall parameter averages, UHF, UB3LYP, and CCSD generally give <50%, ≈90%, and 110%–130% of the shifts predicted by CCSD(T) theory.

The transition state for hydrogen atom dissociation in methoxy (Fig. 1) arises by stretching the unique, longer C–H bond in the $^2A'$ equilibrium structure. Along this path, orbital symmetry is conserved; however, there is a dramatic transformation of the singly occupied, oxygen-localized $7a'$ orbital of methoxy to an isolated hydrogen 1s orbital, while the σ(C–H_3) pair forms the π bond in formaldehyde. The $^2A''$ state of methoxy does not correlate to a low-lying product state and thus rises to much higher energy once $[H\text{–}CH_2O]^{\dagger}(\tilde{X}^2A')$ is reached. In our (best) TZ2P(f,d) RCCSD(T) predictions, R(C–H_3) is extended by 0.679 Å in the transition state. The accompanying changes in

TABLE I. Geometric structures[a] along the $CH_3O \rightarrow CH_2O+H$ fragmentation path given by some recent high-level theoretical studies.

	Ref.	d(C–O)	r(C–$H_{1,2}$)	R(C–H_3)	β($H_{1,2}$–C–O)	δ(H_3–C–O)	γ(H_1–C–H_2)
$CH_3O(\tilde{X}^2A')$ reactant							
TZP MCSCF	33	1.383	1.086	1.111	111.7	106.1	108.1
6-31G* CASSCF	41	1.421	1.085	1.085	111.2	105.7	109.0
DZP CASSCF	34	1.412	1.092	1.092	111.7	105.3	111.5
6-31+G** QCISD	36	1.390		1.110			
cc-pVTZ MR CISD	30	1.3934	1.0876	1.0923	112.3	105.3	107.9
TZ2P(f,d) RCCSD(T)	b	1.3741	1.1026	1.1113	112.92	106.83	111.58
$CH_3O(\tilde{X}^2A'')$ pseudorotated reactant							
cc-pVTZ MR CISD	30	1.3934	1.0904	1.0867	108.3	113.4	110.3
TZ2P(f,d) RCCSD(T)	b	1.3752	1.1071	1.1011	108.55	114.17	104.75
$[H–CH_2O]^{\dagger}(\tilde{X}^2A')$ transition state							
TZP MCSCF	33	1.232	1.087	1.710	120.5	102.5	
DZP CASSCF	34	1.259	1.094	1.668	120.3	102.2	117.1
6-31+G** QCISD	36	1.241		1.661			
TZ2P(f,d) RCCSD(T)	b	1.2263	1.1091	1.7900	121.47	103.29	116.26
$CH_2O(\tilde{X}^1A')+H(^2S)$ product							
TZP MCSCF	33	1.202	1.090	∞	121.5	-	117.0
DZP CASSCF	34	1.226	1.097	∞	121.4	-	117.1
6-31+G** QCISD	36	1.224		∞		-	
cc-pCVQZ CCSD(T)	92	1.2043	1.1008	∞	121.78	-	116.44
TZ2P(f,d) CCSD(T)	b	1.2089	1.1130	∞	121.84	-	116.32
Empirical (r_e)	92	1.2047	1.1007	∞	121.63	-	116.74
Experimental (r_e)[c]	107	1.203	1.099	∞	121.75	-	116.5

[a]Bond lengths in Å and angles in deg. See Fig. 1 for labeling conventions.
[b]Best predictions from current study.
[c]See also Refs. 99 and 108.

r(C–$H_{1,2}$), d(C–O), γ(H_1–C–H_2), and δ(H_3–C–O) are +0.0065 Å, −0.1478 Å, +4.68°, and −1.89°, respectively, the former three quantities exhibiting 86%, 89%, and 98% of their variation for the entire reaction. Clearly, the hydrogen atom dissociation col is a classic, late transition state. As defined in Fig. 1, the angle (ρ) of the C–O bond out of the H_1–C–H_2 plane is only 8.6°, and the deflection angle (θ) of the C–H_3 vector from the normal to the H_1–C–H_2 plane is only 4.7°.

There is wide variation among theoretical predictions of the critical R(C–H_3) distance in the transition state, both in Table I and Fig. 1. The previous MCSCF (Refs. 33 and 34) and QCISD (Ref. 36) distances are 0.08–0.13 Å smaller than our TZ2P(f,d) RCCSD(T) values of 1.79 Å, obtained with a larger basis set and with a more extensive treatment of electron correlation. At the transition state there is severe spin contamination in the UHF reference wave function, as $\langle S^2 \rangle = 0.92$. Accordingly, the UCCSD value for R(C–H_3) is 0.035 Å larger than that for RCCSD, but at the CCSD(T) level this difference is merely 0.0009 Å, indicating the removal of the last vestiges of spin contamination. Most striking in Fig. 1 is the apparent failure of UB3LYP in predicting an anomalously long R(C–H_3) distance of 1.966 Å. In the transition state the pattern among the theoretical values is the same as in the ground-state manifold for the C–$H_{1,2}$ bonds, but not for the C–O bond, where now, more typically, UHF gives d(C–O) smaller than CCSD, and the CCSD →CCSD(T) effect is +0.006 Å. The apparent underestimation of d(C–O) by UB3LYP is still observed, however. The range of γ(H_1–C–H_2) values in the transition state is identical to that at equilibrium, but the order is entirely different. All coupled-cluster values for the aforementioned out-of-plane (ρ) and deflection (θ) angles in the transition state, which specify critical orientations, are tightly grouped in 0.7° ranges. The UHF and UB3LYP (ρ,θ) values lies outside these ranges by (+0.6°,−3.9°) and (−2.9°,+4.6°), respectively, indicating the difficulties of computing these orientational angles at lower levels of theory.

The formaldehyde product ensues from the $[H–CH_2O]^{\dagger}(\tilde{X}^2A')$ transition state via relaxations [at the TZ2P(f,d) RCCSD(T) level] in r(C–$H_{1,2}$), d(C–O), and γ(H_1–C–H_2) of only +0.001 Å, −0.017 Å, and +0.1°, respectively, accompanied by an 8.6° depyramidalization about the carbon atom. Therefore, all of the product vibrational modes, perhaps excepting the $\nu_4(b_1)$ out-of-plane wag, should be highly conserved in the egress from the transition state. Accurate r_e parameters for formaldehyde have very recently been derived by a convolution of empirical rotational constants and cc-pCVQZ CCSD(T) vibrational corrections,[92] along the lines of earlier anharmonic force field studies.[99–101] Comparison of this standard with our values (Table I) reveals C–H and C–O bond length inaccuracies of +0.012 Å and +0.004 Å, respectively, at the TZ2P(f,d) RCCSD(T) level, residual errors which are likely to be roughly constant for all the structures reported here. The corresponding bond angle discrepancies for formaldehyde are at most a few tenths of a degree. Finally, in arriving at the CH_2O product, there are no longer any atypical patterns among the theoretical geometric parameters (Fig. 1); N.B., for d(C–O) the (HF, B3LYP, CCSD) distances are (−0.032, −0.010,−0.007) Å removed from the CCSD(T) value of 1.209 Å.

TABLE II. TZ2P(f,d) harmonic vibrational frequencies (in cm^{-1}) of stationary structures along the $CH_3O \rightarrow CH_2O+H$ fragmentation path.

	UHF	UB3LYP	UCCSD	RCCSD	UCCSD(T)	RCCSD(T)
$CH_3O(\tilde{X}^2A')$ reactant						
$\omega_1(a')H_1-C-H_2$ sym str	3196	2961	3003	3003	2974	2974
$\omega_2(a')C-H_3$ str	3134	2886	2925	2926	2891	2891
$\omega_3(a')H_1-C-H_2$ scissor	1636	1513	1507	1507	1493	1493
$\omega_4(a')H_1-C-H_2$ wag	1553	1364	1381	1382	1360	1360
$\omega_5(a')C-O$ str	1198	1106	1122	1123	1105	1105
$\omega_6(a')O-C-H_3$ bend	1091	958	974	975	956	956
$\omega_7(a'')H_1-C-H_2$ asym str	3216	3005	3046	3045	3020	3020
$\omega_8(a'')H_1-C-H_2$ twist	1558	1355	1381	1380	1362	1364
$\omega_9(a'')H_1-C-H_2$ rock	811	684	754	752	746	745
$CH_3O(\tilde{X}^2A'')$ pseudorotated reactant						
$\omega_1(a')H_1-C-H_2$ sym str	3211	3015	3049	3046	3021	3021
$\omega_2(a')C-H_3$ str	3137	2907	2939	2939	2908	2908
$\omega_3(a')H_1-C-H_2$ scissor	1612	1489	1483	1483	1468	1468
$\omega_4(a')H_1-C-H_2$ wag	1535	1339	1360	1361	1339	1339
$\omega_5(a')C-O$ str	1278	1182	1191	1191	1177	1176
$\omega_6(a')O-C-H_3$ bend	1135	1044	1059	1059	1041	1041
$\omega_7(a'')H_1-C-H_2$ asym str	3198	2935	2991	2992	2959	2962
$\omega_8(a'')H_1-C-H_2$ twist	1603	1408	1435	1434	1421	1423
$\omega_9(a'')H_1-C-H_2$ rock	864i	642i	762i	760i	743i	742i
$[H-CH_2O]^{\dagger}(\tilde{X}^2A')$ transition state						
$\omega_1(a')H_1-C-H_2$ sym str	3135	2887	2927	2924	2894	2894
$\omega_2(a')C-H_3$ str	998i	592i	961i	1018i	962i	947i
$\omega_3(a')H_1-C-H_2$ scissor	1520	1516	1510	1512	1496	1492
$\omega_4(a')H_1-C-H_2$ wag	1220	1168	1183	1190	1171	1165
$\omega_5(a')C-O$ str	1679	1725	1681	1691	1663	1651
$\omega_6(a')O-C-H_3$ bend	505	356	465	485	464	464
$\omega_7(a'')H_1-C-H_2$ asym str	3227	2942	2996	2993	2960	2961
$\omega_8(a'')H_1-C-H_2$ twist	656	401	556	575	544	546
$\omega_9(a'')H_1-C-H_2$ rock	1338	1254	1256	1256	1242	1240
$CH_2O(\tilde{X}^1A')+H(^2S)$ product						
$\omega_1(a_1)H_1-C-H_2$ sym str	3090	2883	2918	2918	2889	2889
$\omega_2(a_1)C-O$ str	1995	1818	1817	1817	1767	1767
$\omega_3(a_1)H_1-C-H_2$ scissor	1651	1533	1535	1535	1518	1518
$\omega_4(b_1)H_1-C-H_2$ wag	1341	1206	1204	1204	1180	1180
$\omega_5(b_2)H_1-C-H_2$ asym str	3161	2943	2988	2988	2958	2958
$\omega_6(b_2)H_1-C-H_2$ rock	1369	1267	1274	1274	1257	1257
Empirical (Ref. 109): $\omega_1=2932$, $\omega_2=1777$, $\omega_3=1535$, $\omega_4=1188$, $\omega_5=3007$, $\omega_6=1272$						

B. Vibrational frequencies

In Table II harmonic vibrational frequencies are presented for the four stationary structures involved in methoxy fragmentation. Note that both the pseudorotated $^2A''$ reactant and the fragmentation transition state display the expected lone imaginary frequencies at all levels of theory. As the nine internal modes of CH_3O evolve during dissociation, the ω_1, ω_2, and ω_5 stretches transform smoothly to product vibrations, the ω_3, ω_4, and ω_9 C–H bending modes experience significant recoupling, and ω_2, ω_6, and ω_8 decay to zero. At the transition state, the $C-H_{1,2}$ stretches exhibit over 90% of their frequency reduction toward formaldehyde, while the C–O stretch, which increases over 650 cm^{-1} overall, displays greater than 80% of its total change. However, in the coupled cluster predictions, the C–O stretch is the only frequency that changes more than 26 cm^{-1} from transition state to product. The $O-C-H_3$ bend and H_1-C-H_2 twist in the transition state have decayed 50%–60% toward free rotations. Clearly, of great concern is the $C-H_3$ barrier frequency (ω^*), which influences the tunneling dynamics of the fragmentation and is quite sensitive to level of theory. Earlier DZP MCSCF (Ref. 33) and DZP CASSCF (Ref. 34) studies provided $\omega^*=1396i$ and $1435i$ cm^{-1}, respectively. At the other extreme, the TZ2P(f,d) UB3LYP value is only $592i$ cm^{-1}. Our best prediction, $\omega^*=947i$ cm^{-1} at the TZ2P(f,d) RCCSD(T) level, supercedes all other values owing to a rigorous treatment of dynamical electron correlation with a robust basis set.

Statistics which characterize the variation of the TZ2P(f,d) frequency predictions in Table II with respect to level of theory are as follows: in relation to the RCCSD(T) standard, the (mean absolute % error, maximum % error in magnitude, % of cases overestimated), among all frequencies except the barrier frequency ω^* of the transition state, is (9.6%, +20.1%, 100%), (3.0%, −26.6%, 47%), and (1.6%, +5.3%, 100%) for UHF, UB3LYP, and RCCSD, respectively. In turn, for formaldehyde the TZ2P(f,d) RCCSD(T) ω_i values uniformly cluster in a very narrow range 0.6%–1.6% below the experimentally derived harmonic frequencies, buttressing confidence in the analogous theoretical pre-

TABLE III. Energetic quantities (in cm^{-1}) for the $CH_3O \rightarrow CH_2O+H$ fragmentation path.

	$\Delta E(^2A''-{}^2A')$	$D_0(D_e)$	$V_0^*(V_e^*)$
This work			
TZ2P(f,d) UHF	28	9295 (11688)	2674 (2337)
TZ2P(f,d) UB3LYP	46	8400 (10491)	840 (541)
TZ2P(f,d) UCCSD	48	6950 (9128)	1974 (1555)
TZ2P(f,d) RCCSD	47	6925 (9103)	2183 (1738)
TZ2P(f,d) UCCSD(T)	51	6146 (8315)	2016 (1583)
TZ2P(f,d) RCCSD(T)	51	6144 (8313)	1907 (1485)
Focal-point[a]		7035 (9204)	1653 (1231)
Previous theory[b,c]			
6-31G**MP3//UHF, Ref. 32		7695	4337
6-31G**QCISD, Ref. 36		9499	1742
TZP MR CI//MCSCF, Ref. 33		6156	2798
cc-pVTZ MR-CCI+Q// DZP CASSCF, Ref. 34		6226	1959
Experiment			
Ref. 47		6900	
Refs. 19, 110		6950±150	1560±150
Ref. 18		6930±200	
RRKM analysis of kinetics; Ref. 12 within Ref. 34			1820, 2170

[a]See Table IV; TZ2P(f,d) RCCSD(T) zero-point vibrational energy corrections utilized.
[b]Results for Jahn–Teller splitting: 42 cm^{-1}, 6-31G**UHF//UMP3 (Ref. 32); 50 cm^{-1}, UMP2 (Ref. 41); 59 cm^{-1}, UMP4 (Ref. 37); 37 cm^{-1}, cc-pVTZ MR CISD (Ref. 30).
[c]A combined $D_0+V_0^*$ value of 8653 cm^{-1} is given by 6-311+G($3df,2p$) QCISD(T)//6-311G(d,p) QCISD theory (Ref. 35).

dictions for the other stationary structures. The UCCSD and UCCSD(T) frequencies for the $(^2A',{}^2A'')$ ground-state manifold all agree with their restricted counterparts within 3 cm^{-1}. In the transition state, where the reference wave function is subject to large spin contamination, the barrier frequency, and to a lesser extent the interfragment bending modes ω_6 and ω_8, are sensitive to the choice of a restricted versus unrestricted coupled-cluster formalism. These same bending modes are the source of the largest differences between the RCCSD(T) frequencies and their RCCSD and UB3LYP counterparts, the latter of which are underestimated by over 20%.

C. Energetics

Table III lists the relative energies corresponding to the TZ2P(f,d) optimum structures in Fig. 1 and compares them with previous theoretical values. All correlated methods yield Jahn–Teller splittings in the 46–51 cm^{-1} range, roughly 20 cm^{-1} larger than the UHF result. These minuscule splittings are in general accord with previous theoretical results[30,32,37,41] (footnote b of Table III), such as the recently reported cc-pVTZ MR CISD value of 37 cm^{-1}.[30] For the $CH_3O \rightarrow CH_2O+H$ dissociation energy, there is an unusual decreasing trend in D_0 with increasing correlation treatment. Specifically, the TZ2P(f,d) UHF→RCCSD→RCCSD(T) sequence is 9295→6925→6144 cm^{-1}. The UCCSD(T) and RCCSD(T) methods agree to 2 cm^{-1}, and both predict $D_0 = 17.6$ kcal mol^{-1}. The analogous TZ2P(f,d) B3LYP value is 6.4 kcal mol^{-1} higher, constituting a considerable overestimation. Among previous theoretical studies,[32–34,36] the cc-pVTZ MR-CCI+Q//DZP CASSCF computations of Walch[34] most closely approach the basis set and correlation requirements for satisfactory convergence, and these results give a dissociation energy 0.23 kcal mol^{-1} larger than that of TZ2P(f,d) RCCSD(T). The association barrier (V_0^*) for the reaction, i.e., the height of the $[H-CH_2O]^{\dagger}(\tilde{X}^2A')$ transition state above CH_2O+H, is the energetic feature of greatest interest here. In Table III it is evident that this small barrier is rather severely underestimated with the TZ2P(f,d) UB3LYP method, by roughly a factor of 2, whereas the analogous UHF result is at least 50% too large. The spurious UB3LYP result may be predominantly due to an anomalous self-energy term for the hydrogen atom asymptote. Compared to D_0, V_0^* is much more sensitive to spin contamination in the reference wave function; the UCCSD→RCCSD V_0^* difference is +209 cm^{-1}, but the UCCSD(T) →RCCSD(T) shift is −109 cm^{-1}. The TZ2P(f,d) RCCSD(T) association barrier, 1907 cm^{-1} or 5.45 kcal mol^{-1}, is 0.15 kcal mol^{-1} smaller than the most reliable previous value of Walch.[34] However, none of the theoretical D_0 and V_0^* values in Table III realistically has an uncertainty less than 1 kcal mol^{-1}, and thus focal-point extrapolations[79–83] are necessary to meaningfully assess (or supersede) experimental measurements.

Our best valence focal-point analyses of the vibrationless dissociation energy and association barrier are detailed in Table IV. For D_e, strong oscillations in the correlation increments are observed, specifically, successive UMP2, UCCSD, and UCCSDT contributions of −18, +12, and −2 kcal mol^{-1}, respectively. However, preliminary cc-pVDZ UBD(TQ) (Ref. 102) computations executed here suggest that the amplitudes of the oscillations past CCSDT are less than 0.1 kcal mol^{-1}. The net, explicitly computed cc-pV5Z UHF, UMP2, and UCCSD dissociation energies differ from their extrapolated limits by only 1, 38, and 15 cm^{-1}, respectively. Using the $X=\{4,5,6\}$, $\{4,5\}$, and $\{4,5\}$ cc-pVXZ UHF,

TABLE IV. Valence focal-point analysis[a] (in cm^{-1}) of the dissociation energy and association barrier for $CH_3O(\tilde{X}^2A')\rightarrow CH_2O(\tilde{X}^1A_1)+H(^2S)$.

	ΔE_e (UHF)	δ[UMP2]	δ[UCCSD]	δ[UCCSD(T)]	δ[UCCSDT]	ΔE_e (UCCSDT)
Dissociation energy (D_e)						
cc-pVDZ(43)	11979	−6570	+3444	−715	+41	8179
cc-pVTZ(102)	12034	−6290	+3902	−858	+114	8902
cc-pVQZ(200)	11959	−6059	+4017	−870	[+114]	[9160]
cc-pV5Z(347)	11974	−6094	+4065	[−870]	[+114]	[9189]
cc-pV6Z(553)	11975	[−6110]	[+4087]	[−870]	[+114]	[9196]
Extrapolation limit (∞)	[11975]	[−6132]	[+4117]	[−870]	[+114]	[9204]
Association barrier (V_e^*)						
cc-pVDZ(43)	2066	+3758	−3597	+76	−139	2164
cc-pVTZ(102)	2031	+3252	−3686	+52	−168	1481
cc-pVQZ(200)	2044	+3175	−3761	+37	[−168]	[1327]
cc-pV5Z(347)	2049	+3160	−3796	[+37]	[−168]	[1282]
cc-pV6Z(553)	2050	[+3153]	[−3812]	[+37]	[−168]	[1261]
Extrapolation limit (∞)	[2050]	[+3144]	[−3833]	[+37]	[−168]	[1231]

[a]The analysis is performed at TZ2P(f,d) UCCSD(T) optimum structures. The symbol δ denotes the increment in the relative energy (ΔE_e) with respect to the preceding level of theory in the correlation series UMF→UMP2→UCCSD→UCCSD(T)→UCCSDT. For each one-particle basis, the total number of contracted Gaussian functions is given in parentheses. The extrapolated UHF, UMP2, and UCCSD entries shown in brackets were obtained via direct fits of Eqs. (1) and (2) to the cc-pVXZ data of highest cardinal number, i.e., $X=\{4,5,6\}$ and $\{4,5\}$ for the UHF and correlation energies, respectively. Simple additivity was assumed for the UCCSD(T) and UCCSDT increments listed in brackets.

UMP2, and UCCSD points, in order, in direct fits to Eqs. (1) and (2), in conjunction with assumed additivity of the smaller-basis coupled-cluster triples increments, yields a final prediction of $D_e=9204$ cm^{-1} (26.3 kcal mol^{-1}), or $D_0=7035$ cm^{-1} (20.1 kcal mol^{-1}) with TZ2P(f,d) RCCSD(T) zero-point vibrational corrections. If the cc-pVTZ points are included in all the fits, D_e is raised by 136 cm^{-1}, but the computed large-X variations are not as uniform or credible. If a separate $X=\{3,4\}$ extrapolation of the UCCSD(T) data is performed, D_e increases by 216 cm^{-1}, but the limiting δ[UCCSD(T)]=−654 cm^{-1} is in clear disagreement with the explicitly computed cc-pVQZ increment of −870 cm^{-1}. One concludes that the cc-pVTZ energies are too far removed from the asymptotic regime to be reliably used in basis set extrapolations for the dissociation energy. If the Hartree–Fock and correlation energies are all extrapolated with the exponential form of Eq. (1), D_e is lowered by 75 cm^{-1}. Finally, if Schwartz4 and Schwartz6 extrapolations[103] are performed, D_e is reduced by 3 and 65 cm^{-1}, respectively. In summary, alternate extrapolation schemes yield results which envelope the value adopted here, $D_e=9204$ cm^{-1}, which is not only a compromise value but is also preferred on the grounds of more credible fits and basis set trends.

The focal-point layout of V_e^* in Table IV displays UMP2, UCCSD, and UCCSDT contributions of +9, −11, and −0.4 kcal mol^{-1}, respectively, i.e., a large MP2 increase of the barrier nullified by a larger UCCSD decrease, followed (unlike the D_e case) by only a small UCCSDT effect. Again, our preliminary cc-pVDZ UBD(TQ) computations suggest that the next increment due to connected quadruple excitations is less than 0.1 kcal mol^{-1}. The net, explicitly computed cc-pV5Z UHF, UMP2, and UCCSD barriers already closely approach their extrapolated limits, within 1, 15, and 52 cm^{-1}, respectively. The same extrapolation scheme preferred for D_e now predicts the final value $V_e^*=1231$ cm^{-1} (3.5 kcal mol^{-1}), or $V_0^*=1653$ cm^{-1} (4.7 kcal mol^{-1}) with TZ2P(f,d) RCCSD(T) zero-point corrections. The alternative extrapolation procedures tested for D_e give results scattered closely about this proposal (within 30 cm^{-1}), indicating much improved consistency in inferring CBS limits. For example, an $X=\{3,4\}$ extrapolation of the UCCSD(T) data gives a credible limit of δ[UCCSD(T)]=+18 cm^{-1} and a barrier decrease of 19 cm^{-1}. On the other hand, performing exponential extrapolations on all the UHF, UMP2, and UCCSD data raises the barrier by 28 cm^{-1}. The preferred focal-point result $V_e^*=3.5$ kcal mol^{-1} is 0.7 kcal mol^{-1} below the TZ2P(f,d) RCCSD(T) barrier, a shift which is energetically significant, but small enough to allay concerns over the optimized geometric structure of the transition state adopted for the focal-point analysis.

IV. DISCUSSION

In a 1995 study, Dertinger and co-workers[19] used SEP techniques to measure rovibrational quantum-state resolved unimolecular dissociation rates [$k(v,J)$] of highly excited methoxy radicals over a 3000 cm^{-1} range of energies enveloping the formaldehyde appearance threshold. A striking degree of quantum-state specificity was observed over the full excitation energy range. For example, in a manifold of 27 neighboring states in the tunneling regime near 7460 cm^{-1}, the decay constants varied by up to two orders of magnitude, and differences by a factor of 8 were witnessed for states only 0.3 cm^{-1} apart. Nonetheless, averages over the erratic variations were taken to infer statistical rate constants $k(E,J)$, which were then fit to a conventional RRKM expression, modified to include hydrogen atom tunneling. The analysis was based on the DZP CASSCF rotational constants and vibrational frequencies for the transition state computed earlier by Walch,[34] except that the imaginary barrier frequency was scaled in the process. The association barrier $V_0^*=1560\pm150$ cm^{-1} (4.5 ± 0.4 kcal mol^{-1}) was adopted from a 1994 investigation (by the same experimental group) of the activation energy for H–D isotope exchange in the reaction $D+H_2CO$. The RRKM analysis of averages over the quantum-state specific rates then provided a dissociation en-

ergy $D_0 = 6950 \pm 150$ cm^{-1} (19.9 ± 0.4 kcal mol^{-1}) and a barrier frequency $\omega^* = 830i$ cm^{-1}. Despite the numerous assumptions made in treating the data, the derived values of D_0 and V_0^* are both in excellent agreement with our final focal-point energetics; as shown in Table III, experiment lies below theory by 0.2–0.3 kcal mol^{-1} in both cases. Finally, the validity of the empirical barrier frequency is confirmed by the TZ2P(f,d) RCCSD(T) prediction ($\omega^* = 947i$ cm^{-1}) mentioned above, especially if anharmonic effects on tunneling through the fragmentation barrier are considered. This accord further vitiates the high barrier frequencies near $1400i$ cm^{-1} given by earlier MCSCF computations[33,34] and the low value of $592i$ cm^{-1} obtained here with the TZ2P(f,d) UB3LYP method.

A consensus on the C–H bond dissociation energy of methoxy and $\Delta H^\circ_{f,0}(CH_3O)$ is provided by the new theoretical data reported here. In 1991, Ruscic and Berkowitz[104] reviewed earlier sources and adopted $\Delta H^\circ_{f,0}(CH_3O) = 5.9 \pm 1.0$ kcal mol^{-1}, and in Chart 3 of a 1994 feature article on experimental methods for the measurement of RH bond energies, Berkowitz, Ellison, and Gutman[105] list $D_0(H–CH_2O) = 21 \pm 1$ kcal mol^{-1}. In 1995, Osborn *et al.*[18] employed fast beam photofragment translational spectroscopy of CH_3O radicals produced by photodetachment of methoxide anions and deduced $D_0 = 19.8 \pm 0.4$ kcal mol^{-1} and $\Delta H^\circ_{f,0}(CH_3O) = 6.8 \pm 0.4$ kcal mol^{-1}, the former value lying within 0.1 kcal mol^{-1} of the result of Dertinger and co-workers.[19] Our final theoretical proposal $D_0 = 20.1$ kcal mol^{-1} is a compromise value nicely lying within the error bars of all three empirical dissociation energies. Assuming the same experimental reference enthalpy used by Osborn *et al.*,[18] $\Delta H^\circ_{f,0}(CH_2O) = -25.0$ kcal mol^{-1}, which is consistent with $\Delta H^\circ_{f,298}(CH_2O)$ in Ref. 106, our $D_0(H–CH_2O)$ translates to $\Delta H^\circ_{f,0}(CH_3O) = 6.5$ kcal mol^{-1}. This heat of formation is again intermediate between and within the error bars of the empirical quantities of Refs. 104 and 18.

The theoretical results reported in this paper provide significant improvements in current knowledge of the features of the potential energy surface for hydrogen atom dissociation from the methoxy radical. In general the uncertainties in our best theoretical predictions are less than those of experiment. Most notably, the C_s-symmetry $^2A'$ transition state for CH_2O+H fragmentation is determined to exhibit a critical distance $R^*(C–H) = 1.79$ Å, a barrier frequency $\omega^* = 947i$ cm^{-1}, a reverse barrier height $V_0^* = 4.7$ kcal mol^{-1}, and a forward barrier height $D_0 + V_0^* = 24.8$ kcal mol^{-1}. The key energetic quantities advanced here are derived from focal-point extrapolations of explicitly computed total energies which certainly lie in the asymptotic regime for basis set convergence in the cc-pVXZ series. In this system, consistent asymptotic behavior was only observed beyond the cc-pVTZ basis set, and thus only $X = 4$, 5, and 6 energy points, involving as many as 553 one-particle functions, were employed in the final extrapolations. It is hoped that these new theoretical data will be a boon to ongoing photofragmentation experiments on CH_3O designed to probe fundamental principles of chemical dynamics.

ACKNOWLEDGMENTS

This research was supported by the U.S. Department of Energy, Office of Basic Energy Sciences, Fundamental Interactions Branch, Grant No. DE-FG02-00ER14748. The authors are grateful to Professor C. B. Moore for motivation and to Dr. D. E. Woon for providing methoxy data prior to publication. N.D.K.P. would like to acknowledge Dr. J. C. Rienstra-Kiracofe, C. Barden, J. Gonzales, C. Pak, and N. Richardson for many valuable discussions.

[1] D. W. Style and J. C. Ward, Trans. Faraday Soc. **49**, 999 (1953).
[2] S. C. Foster and T. A. Miller, J. Phys. Chem. **93**, 5986 (1989).
[3] C. K. Westbrook and F. L. Dryer, Prog. Energy Combust. Sci. **10**, 1 (1984).
[4] B. A. Williams and J. W. Flemming, Chem. Phys. Lett. **221**, 27 (1994).
[5] S. Zabarnick, Combust. Flame **85**, 27 (1991).
[6] B. J. Finlayson and J. N. Pitts, *Atmospheric Chemistry* (Wiley, New York, 1986).
[7] D. G. Hendry, J. Phys. Chem. **81**, 2483 (1977).
[8] A. C. Aikin, J. Geophys. Res. **87**, 3105 (1982).
[9] D. Perner, U. Platt, M. Trainer, *et al.*, J. Atmos. Chem. **5**, 185 (1987).
[10] H. Heicklen, K. Westberg, and N. Cohen (unpublished).
[11] T. Baer and W. L. Hase, *Unimolecular Reaction Dynamics. Theory and Experiments* (Oxford University Press, New York, 1996).
[12] R. G. Gilbert and S. C. Smith, *Theory of Unimolecular and Recombination Reactions* (Blackwell, Oxford, 1990).
[13] M. M. Kreevoy and D. G. Truhlar, in *Investigations of Rates and Mechanisms of Reactions*, edited by C. F. Bernasconi (Wiley, New York, 1986), Vol. 6, P. 1, p. 13.
[14] C. S. Parmenter, Faraday Discuss. R. Soc. Chem. **75**, 7 (1983).
[15] A. E. W. Knight, in *Excited States*, edited by E. C. Lin and K. K. Innes (Academic, San Diego, 1988).
[16] L. R. Khundkar and A. H. Zewail, Annu. Rev. Phys. Chem. **41**, 15 (1990).
[17] D. L. Osborn, D. J. Leahy, and D. M. Neumark, J. Phys. Chem. A **101**, 6583 (1997).
[18] D. L. Osborn, D. J. Leahy, E. R. Ross, and D. M. Neumark, Chem. Phys. Lett. **235**, 484 (1995).
[19] S. Dertinger, A. Geers, J. Kappert, J. W. Wiebrecht, and F. Temps, Faraday Discuss. R. Soc. Chem. **102**, 31 (1995).
[20] A. Geers, J. Kappert, F. Temps, and J. W. Wiebrecht, Ber. Bunsenges. Phys. Chem. **94**, 1219 (1990).
[21] E. R. Lovejoy, S. K. Kim, and C. B. Moore, Science **256**, 1541 (1992).
[22] S. K. Kim, E. R. Lovejoy, and C. B. Moore, J. Chem. Phys. **102**, 3202 (1995).
[23] R. A. King, W. D. Allen, B. Ma, and H. F. Schaefer III, Faraday Discuss. Chem. Soc. **110**, 23 (1998).
[24] J. D. Gezelter and W. H. Miller, J. Chem. Phys. **104**, 3546 (1996).
[25] Q. Cui and K. Morokuma, J. Chem. Phys. **107**, 4951 (1997).
[26] G.-H. Leu, C.-L. Huang, S.-H. Lee, Y.-C. Lee, and I.-C. Chen, J. Chem. Phys. **109**, 9340 (1998).
[27] R. A. King, W. D. Allen, and H. F. Schaefer III, J. Chem. Phys. **112**, 5585 (2000).
[28] H. A. Jahn and E. Teller, Proc. R. Soc. London, Ser. A **161**, 220 (1937).
[29] G. Herzberg, *Electronic Spectra and Electronic Structure of Polyatomic Molecules* (Van Nostrand Reinhold, New York, 1966).
[30] U. Höper, P. Botschwina, and H. Köppel, J. Chem. Phys. **112**, 4132 (2000).
[31] D. R. Yarkony, H. F. Schaefer, and S. Rothenberg, J. Am. Chem. Soc. **96**, 656 (1974).
[32] S. Saebø, L. Radom, and H. F. Schaefer, J. Chem. Phys. **78**, 845 (1983).
[33] M. Page, M. C. Lin, Y. He, and T. K. Choudhury, J. Phys. Chem. **93**, 4404 (1989).
[34] S. P. Walch, J. Chem. Phys. **98**, 3076 (1993).
[35] H. Hippler, F. Stribel, and B. Viskolcz, Phys. Chem. Chem. Phys. **3**, 2450 (2001).
[36] D. E. Woon Astrophys. J. **569**, 541 (2002).
[37] G. D. Bent, G. F. Adams, R. H. Bartram, G. D. Purvis, and R. J. Bartlett, J. Chem. Phys. **76**, 4144 (1982).

[38] S. M. Colwell, R. D. Amos, and N. C. Handy, Chem. Phys. Lett. **109**, 525 (1984).
[39] L. A. Curtiss, L. D. Kock, and J. A. Pople, J. Chem. Phys. **95**, 4040 (1991).
[40] J. T. Carter and D. B. Cook, J. Mol. Struct.: THEOCHEM **251**, 111 (1991).
[41] T. A. Barkholtz and T. A. Miller, J. Phys. Chem. A **103**, 2321 (1999).
[42] L. Blatt, Int. J. Chem. Kinet. **11**, 977 (1979).
[43] G. B. Ellison, P. C. Engelking, and W. C. Lineberger, J. Phys. Chem. **86**, 4873 (1982).
[44] D. F. McMillen and D. M. Golden, Annu. Rev. Phys. Chem. **33**, 493 (1982).
[45] J. L. Holmes and F. P. Lossing, Int. J. Mass Spectrom. Ion Processes **58**, 113 (1984).
[46] R. Atkinson, D. L. Baulch, R. A. Cox, R. F. Hampton, J. A. Kerr, and J. Troe, J. Phys. Chem. Ref. Data **21**, 1125 (1992).
[47] A. Geers, J. Kappert, F. Temps, and J. W. Wiebrecht, J. Chem. Phys. **99**, 2271 (1993).
[48] A. Geers, J. Kappert, and F. Temps, J. Chem. Phys. **98**, 4297 (1993).
[49] A. Geers, J. Kappert, F. Temps, and J. W. Wiebrecht, J. Chem. Phys. **101**, 3618 (1994).
[50] A. Geers, J. Kappert, F. Temps, and J. W. Wiebrecht, J. Chem. Phys. **101**, 3634 (1994).
[51] W. J. Hehre, L. Radom, P. v. R. Schleyer, and J. A. Pople, *Ab Initio Molecular Orbital Theory* (Wiley-Interscience, New York, 1986).
[52] C. C. J. Roothaan, Rev. Mod. Phys. **23**, 69 (1951).
[53] J. A. Pople and R. K. Nesbet, J. Chem. Phys. **22**, 571 (1954).
[54] A. Szabo and N. S. Ostlund, *Modern Quantum Chemistry: Introduction to Advanced Electronic Structure Theory*, 1st ed., revised (McGraw-Hill, New York, 1989).
[55] S. Saebø and J. Almlöf, Chem. Phys. Lett. **154**, 83 (1989).
[56] M. Head-Gordon, J. A. Pople, and M. J. Frisch, Chem. Phys. Lett. **153**, 503 (1988).
[57] G. E. Scuseria, A. C. Scheiner, T. J. Lee, J. E. Rice, and H. F. Schaefer III, J. Chem. Phys. **86**, 2881 (1987).
[58] A. C. Scheiner, G. E. Scuseria, J. E. Rice, T. J. Lee, and H. F. Schaefer III, J. Chem. Phys. **87**, 5361 (1987).
[59] R. J. Bartlett, Annu. Rev. Phys. Chem. **32**, 359 (1981).
[60] R. J. Bartlett, C. E. Dykstra, and J. Paldus, in *Advanced Theories and Computational Approaches to the Electronic Structure of Molecules*, edited by C. E. Dykstra (Reidel, Dordrecht, 1983), p. 127.
[61] G. E. Scuseria and H. F. Schaefer III, Chem. Phys. Lett. **152**, 382 (1988).
[62] J. Noga and R. J. Bartlett, J. Chem. Phys. **86**, 7041 (1987).
[63] J. Noga and R. J. Bartlett, J. Chem. Phys. **89**, 3401 (1988).
[64] K. Raghavachari, G. W. Trucks, J. A. Pople, and M. Head-Gordon, Chem. Phys. Lett. **157**, 479 (1989).
[65] G. E. Scuseria and T. J. Lee, J. Chem. Phys. **93**, 5851 (1990).
[66] J. F. Stanton, J. Gauss, J. D. Watts, W. J. Lauderdale, and R. J. Bartlett, ACESII, 1993. The package also contains modified versions of the MOLECULE Gaussian integral program of J. Almlöf and P. R. Taylor, the ABACUS integral derivative program written by T. U. Helgaker, H. J. Aa. Jensen, P. Jørgensen, and P. R. Taylor, and the PROPS property evaluation integral code of P. R. Taylor.
[67] A. D. Becke, J. Chem. Phys. **98**, 5648 (1993).
[68] C. Lee, W. Yang, and R. G. Parr, Phys. Rev. B **37**, 785 (1988).
[69] M. J. Frisch, G. W. Trucks, M. Head-Gordon, GAUSSIAN 94, revision C Gaussian, Inc., Pittsburgh, PA, 1995.
[70] S. Huzinaga, J. Chem. Phys. **42**, 1293 (1965).
[71] T. H. Dunning, Jr., J. Chem. Phys. **53**, 2823 (1970).
[72] T. H. Dunning, Jr. and P. J. Hay, in *Modern Theoretical Chemistry*, edited by H. F. Schaefer III (Plenum, New York, 1977), Vol. 3, pp. 1–27.
[73] T. H. Dunning, Jr., J. Chem. Phys. **90**, 1007 (1989).
[74] T. H. Dunning, Jr., J. Chem. Phys. **55**, 716 (1971).
[75] D. E. Woon and T. H. Dunning, Jr., J. Chem. Phys. **98**, 1358 (1993).
[76] Y. Yamaguchi, Y. Osamura, J. D. Goddard, and H. F. Schaefer III, *A New Dimension to Quantum Chemistry: Analytic Derivative Methods in Ab initio Molecular Electronic Structure Theory* (Oxford University Press, New York, 1994).
[77] J. Gauss, W. J. Lauderdale, J. F. Stanton, J. D. Watts, and R. J. Bartlett, Chem. Phys. Lett. **182**, 207 (1991).
[78] J. D. Watts, J. Gauss, and R. J. Bartlett, J. Chem. Phys. **98**, 8718 (1993).
[79] A. G. Császár, W. D. Allen, and H. F. Schaefer III, J. Chem. Phys. **108**, 9751 (1998).
[80] A. L. L. East and W. D. Allen, J. Chem. Phys. **99**, 4638 (1993).
[81] W. D. Allen, A. L. L. East, and A. G. Császár, in *Structures and Conformations of Non-Rigid Molecules*, edited by J. Laane, M. Dakkouri, B. van der Veken, and H. Oberhammer (Kluwer, Dordrecht, 1993).
[82] E. F. Valeev, W. D. Allen, H. F. Schaefer III, A. G. Császár, and A. L. L. East, J. Phys. Chem. A **105**, 2716 (2001).
[83] G. Tarczay, A. G. Császár, W. Klopper, V. Szalay, W. D. Allen, and H. F. Schaefer III, J. Chem. Phys. **110**, 11971 (1999).
[84] A. K. Wilson, T. van Mourik, and T. H. Dunning, Jr., J. Mol. Struct.: THEOCHEM **388**, 339 (1996).
[85] K. A. Peterson, R. A. Kendall, and T. H. Dunning, Jr., J. Chem. Phys. **99**, 1930 (1993).
[86] K. A. Peterson, R. A. Kendall, and T. H. Dunning, Jr., J. Chem. Phys. **99**, 9790 (1993).
[87] D. Feller, J. Chem. Phys. **96**, 6104 (1992).
[88] D. Feller, J. Chem. Phys. **98**, 7059 (1993).
[89] T. Helgaker, W. Klopper, H. Koch, and J. Noga, J. Chem. Phys. **106**, 9639 (1997).
[90] W. Kutzelnigg and J. D. Morgan III, J. Chem. Phys. **96**, 4484 (1992).
[91] W. Kutzelnigg and J. D. Morgan III, J. Chem. Phys. **97**, 8821 (1992).
[92] K. L. Bak, J. Gauss, P. Jørgensen, J. Olsen, T. Helgaker, and J. F. Stanton, J. Chem. Phys. **114**, 6548 (2001).
[93] T. J. Lee and G. E. Scuseria, in *Quantum Mechanical Electronic Structure Calculations with Chemical Accuracy*, edited by S. R. Langhoff (Kluwer, Dordrecht, 1995), p. 47.
[94] R. J. Bartlett, J. Phys. Chem. **93**, 1697 (1989).
[95] T. D. Crawford and H. F. Schaefer, Rev. Comput. Chem. **14**, 33 (2000).
[96] J. Paldus and X. Li, Adv. Chem. Phys. **101**, 1 (1999).
[97] J. M. Gonzales, R. S. Cox III, S. T. Brown, W. D. Allen, and H. F. Schaefer III, J. Phys. Chem. A **105**, 11327 (2001).
[98] T. Momose, Y. Endo, E. Hirota, and T. Shida, J. Chem. Phys. **88**, 5338 (1988).
[99] D. A. Clabo, Jr., W. D. Allen, R. B. Remington, Y. Yamaguchi, and H. F. Schaefer III, Chem. Phys. **123**, 187 (1988).
[100] A. L. L. East, C. S. Johnson, and W. D. Allen, J. Chem. Phys. **98**, 1299 (1993).
[101] A. L. L. East, W. D. Allen, and S. J. Klippenstein, J. Chem. Phys. **102**, 8506 (1995).
[102] K. Raghavachari, J. A. Pople, E. S. Replogle, and M. Head-Gordon, J. Phys. Chem. **94**, 5579 (1990).
[103] J. M. L. Martin, Chem. Phys. Lett. **259**, 669 (1996).
[104] B. Ruscic and J. Berkowitz, J. Chem. Phys. **95**, 4033 (1991).
[105] J. Berkowitz, G. B. Ellison, and D. Gutman, J. Phys. Chem. **98**, 2744 (1994).
[106] J. Cioslowski, M. Schimeeczek, G. Liu, and V. Stoyanov, J. Chem. Phys. **113**, 9377 (2000).
[107] K. Yamada, T. Nakagawa, K. Kuchitsu, and Y. Morino, J. Mol. Spectrosc. **38**, 70 (1971).
[108] J. L. Duncan, Mol. Phys. **28**, 1177 (1974).
[109] D. C. Burleigh, A. B. McCoy, and E. L. Sibert III, J. Chem. Phys. **104**, 480 (1996).
[110] S. Dóbé, C. Oehlers, F. Temps, H. G. Wagner, and H. Ziemer, Ber. Bunsenges. Phys. Chem. **98**, 754 (1994).